

Hydrogen absorption of nanoscale Pd particles embedded in ZrO₂ matrix prepared from Zr–Pd amorphous alloys

Shin-ichi Yamaura,^{a)} Ken-ichiro Sasamori, Hisamichi Kimura, and Akihisa Inoue
Institute for Materials Research, Tohoku University, 2-1-1 Katahira, Aoba, Sendai 980-8577, Japan

Yue Chang Zhang and Yoshiaki Arata
Osaka University, 11-1 Mihogaoka, Ibaraki, Osaka 567-0047, Japan

(Received 27 November 2001; accepted 11 March 2002)

Nanocomposite materials consisting of ZrO₂ and Pd phases were prepared by heating the amorphous Zr₆₅Pd₃₅ alloy for 24 h at 553 K in air. The maximum hydrogen absorption amount is about 2.4 mass% (H₂/Pd) at 323 K and 2.2 mass% (H₂/Pd) at 423 K at hydrogen pressure of 1 MPa. The absorption amount of Pd nanoparticles in the nanocomposite is a few times larger than those for the bulk and powder Pd metals. The remarkable increase in the hydrogen absorption/desorption amounts seems to result from the isolated dispersion state of Pd nanoparticles in the ZrO₂ phase containing a tremendously large interface area in the nanocomposite.

I. INTRODUCTION

Recently, nanostructured materials have attracted rapidly increasing interest because of anomalous effects caused by the nanometer-scale structure. Amorphous alloys containing large amounts of solute elements have been regarded as one of the best starting materials to fabricate nanoscale mixed materials. In 1992, some of the present authors have reported that the oxidation of Zr–M (M = Cu, Ni, Pd) binary amorphous alloys in air leads to the synthesis of nanoscale composite materials in which nanoscale metallic (M) particles are distributed and embedded isolately in a monoclinic and cubic ZrO₂ matrix.^{1,2} For instance, the Pd particles in a ZrO₂ phase prepared from an amorphous Zr₆₅Pd₃₅ alloy have a spherical morphology with an average diameter of 10 nm and distribute homogeneously in an isolated state. Subsequently, we have performed a number of studies on the formation mechanism of the novel nanoscale mixed structure and various characteristics such as catalytic effects³ and mechanical properties⁴ of the mixed materials for the past 1 decade.

In general, there are two stages in the process of hydrogen absorption of hydrogen storage materials such as Pd. The first stage of absorption is the solution of hydrogen into the α phase, and the second stage, the hydrogenation of the material itself, accompanying the change from α phase (Pd) to β phase (Pd hydride). There have been experimental and theoretical studies on hydrogen absorption of nanoscale Pd particles.^{5,6}

Zuettel *et al.* reported that hydrogen absorption of solitary nanoscale Pd clusters decreased with a decrease of cluster size.⁵ Pundt *et al.* studied hydrogen absorption of the composite material consisting of isolated Pd clusters dispersed in a polymer matrix and reported that hydrogen solubility of the composite material increased and the miscibility gap became narrower as compared with those of the bulk Pd metal.⁶ Moreover, hydrogen absorption studies on Pd nanocrystals have also been performed.^{7,8} Eastman *et al.* showed that the hydrogen solubility of nanocrystalline and coarse-grained Pd metals increased with decreasing grain size and the miscibility gap of Pd nanocrystals was smaller than that of the Pd bulk.⁸ From these results, it can be concluded that the hydrogen absorption properties of nanoscale Pd particles strongly depend on the surface condition of the particles. However, little is known about the effect of dispersed Pd particles in the ZrO₂ phase on hydrogen absorption characteristics. There have been some data on the enhancement of hydrogen absorption characteristics for mechanically alloyed materials in Mg-based alloy systems.⁹ The origin for the enhancement has been attributed to an increase in the specific surface ratio through the refinements of sample morphology and structure, though the resulting finely mixed phases were subjected to contamination caused by mechanical alloying. On the other hand, the nanoscale metallic particles embedded in ZrO₂ produced by oxidation in air have been thought to have a characteristic interface because of the preferential oxidation effect of Zr element and spontaneous condensation of Pd element as a particle form.^{1,2} It is therefore expected that the nanoscale Pd particles lead to an enhancement of hydrogen absorption

^{a)}Address all correspondence to this author.

characteristics as compared with ordinary Pd metal in bulk and powder forms. This paper intends to study the hydrogen absorption characteristics of the nanoscale ZrO₂ + Pd composite material produced by oxidizing the rapidly solidified Zr₆₅Pd₃₅ amorphous alloy.

II. EXPERIMENTAL PROCEDURE

Binary and ternary alloys with compositions of Zr₆₅Pd₃₅, Zr₇₀Au₃₀, and Zr₆₅Pd₃₀Ni₅ were examined in this study. Their alloy ingots were prepared from the mixtures of pure Zr, Pd, Au, and Ni metals by arc melting in an Ar atmosphere. Amorphous alloy ribbons with a cross section of about 0.02 × 1.5 mm² were produced by melt spinning in an Ar atmosphere from the alloy ingot. Thermal stability of as-spun specimens was also measured by differential scanning calorimetry (DSC), thermogravimetric analysis (TGA), and differential thermal analysis (DTA).

Ribbon specimens were oxidized at 553 K for 24 h in static air. The structures in as-spun and oxidized ribbons were examined by x-ray diffraction (XRD) using copper radiation (Cu K_α) obtained at 35 kV and 15 mA. X-ray diffraction data were collected over the angular range of 2θ = 20°–80°. Transmission electron microscopy (TEM) images of the oxidized specimens were obtained by using well-pulverized powders of the specimen.

Hydrogen absorption properties were evaluated by measuring the hydrogen pressure–concentration (hereafter denoted as *P*–*C*) isotherms with the gas-volumetric (Sieverts) apparatus at 323 and 423 K.

III. RESULTS AND DISCUSSION

A. Thermal stability of amorphous alloys in air and Ar atmospheres

Figure 1 shows the thermal analysis data obtained by DSC, TGA, and DTA. Figure 1(a) shows a DSC curve of the as-spun Zr₆₅Pd₃₅ alloy in an Ar atmosphere. Two exothermic peaks are seen, indicating that the crystallization occurs through two stages. It has been reported that the first and second exothermic peaks correspond to the phase transitions from an amorphous to a tetragonal Zr₂Pd compound and from the remaining amorphous phase to hcp Zr plus tetragonal Zr₂Pd phases, respectively.² Figure 1(b) indicates DTA and TGA curves of the as-spun Zr₆₅Pd₃₅ alloy heated in air. A broad exothermic peak starts at about 600 K that is much lower than the onset temperature of crystallization (750 K) in an Ar atmosphere. It is also seen that the weight begins to increase around 600 K. It is therefore concluded that the broad exothermic reaction in the temperature range above 600 K is due to the oxidation of the alloy. It is important to point out that the oxidation begins to occur at temperatures much below the crystallization temperature. This indicates that the long-time oxidation at the

temperatures below crystallization temperature causes an ultrafine mixed structure consisting of nanoscale Pd particles dispersed in ZrO₂ matrix produced directly from the amorphous phase through the preferential oxidation of Zr rather than Pd in the Zr–Pd amorphous alloy without an intermediate stage of a crystallized alloy phase, as previously reported by some of the present authors.^{1,2}

B. Microstructure

Figures 2(a) and 2(b) show the XRD patterns of the Zr₆₅Pd₃₅ alloy in the as-spun state and the oxidized state in air at 553 K for 24 h, respectively. The as-spun alloy

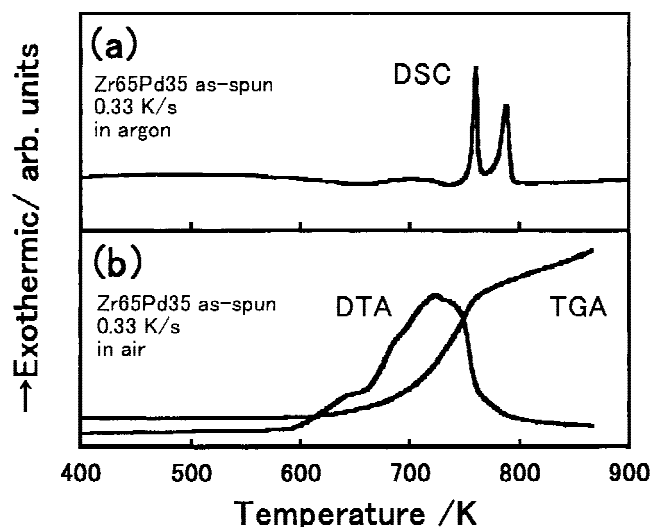


FIG. 1. (a) DSC curve of the melt-spun Zr₆₅Pd₃₅ amorphous alloy ribbon measured in an argon atmosphere. (b) DTA and TGA curves of the melt-spun Zr₆₅Pd₃₅ amorphous alloy ribbon measured in static air.

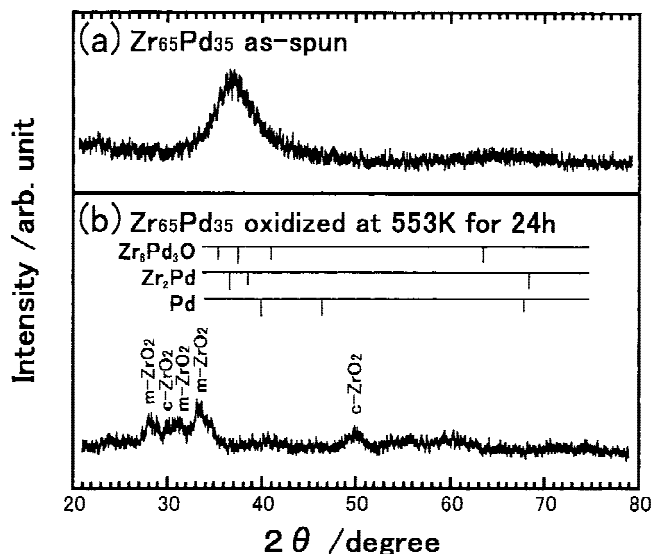


FIG. 2. X-ray diffraction patterns of the melt-spun Zr₆₅Pd₃₅ alloy: (a) as-spun state; (b) annealed state at 553 K for 24 h in air.

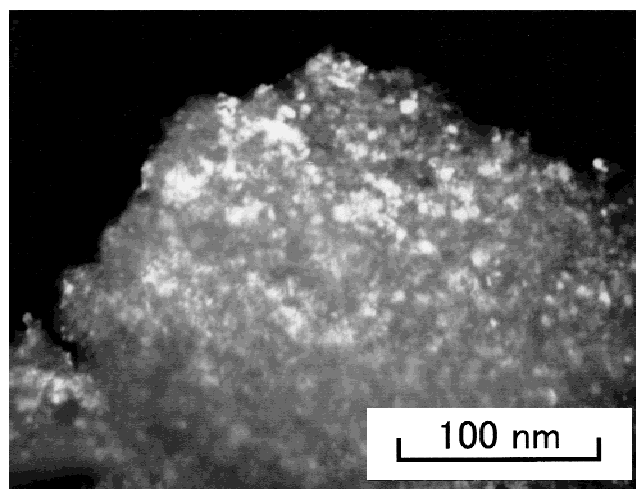
consists of an amorphous single phase, and the heating in air results in the change to a mixed structure consisting of monoclinic and cubic ZrO₂ phases. No distinct other phase is seen. The absence of Pd diffraction peaks is presumably due to extremely small particle sizes of the Pd phase.

Figure 3 shows dark-field TEM image and selected-area electron diffraction pattern of the Zr₆₅Pd₃₅ amorphous alloy heated at 553 K for 24 h in air, together with analytical data of the diffraction pattern. The dark-field image was taken from a part of (111) Pd reflection ring. As identified in Fig. 3, the oxidized structure consists of monoclinic ZrO₂, cubic ZrO₂, and fcc Pd phases. From the rough estimation, the volume fraction of Pd particles is about 20%. The Pd particle size is measured to be about 10 nm.

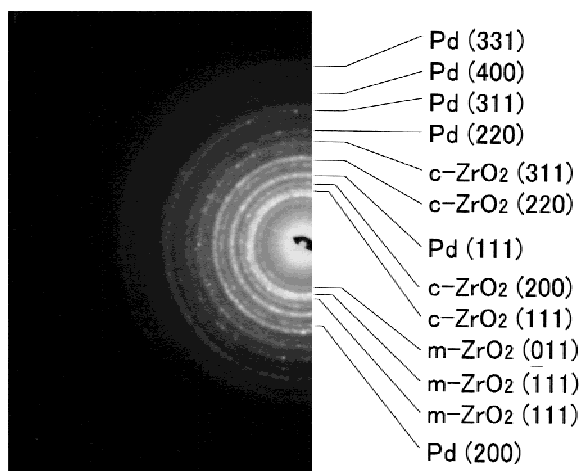
It is known that Zr₂Pd itself possesses high hydrogen absorption ability.^{10,11} However, the Zr₂Pd phase cannot be detected in the present XRD and TEM data, as demonstrated in Figs. 2 and 3. The oxidation-induced structure of the Zr₆₅Pd₃₅ amorphous alloy consists of monoclinic and cubic ZrO₂ and fcc Pd phases which resulted from the preferential oxidation of Zr element in the amorphous phase. It has previously been reported that some Zr–M–O (M = metal) ternary compounds such as Zr₄Pd₂O can also absorb hydrogen.^{12–16} However, the present structural data did not reveal any evidence of the formation of the Zr–Pd–O ternary compound as shown in Fig. 2. The Zr₆Pd₃O and Zr₄Pd₂O phases would show the same diffraction patterns since the Zr₆Pd₃O phase has the same big-cube structure with a lattice constant of 1.2458 nm as that of the Zr₄Pd₂O phase. We cannot find any sharp peaks around 37° and 63° in Fig. 2. In addition, it may be difficult to synthesize these ternary compounds by oxidation in air because the precise control of oxygen content is required to synthesize the multicomponent compounds directly from the mixture of component metals.¹⁷ Therefore, it is concluded that the contribution of Zr₂Pd and Zr₄Pd₂O compounds to the present hydrogen absorption data can be neglected.

C. Hydrogen absorption of ZrO₂ + Pd nanocomposites

We have also confirmed the formation of a similar nanocomposite structure consisting of monoclinic ZrO₂, cubic ZrO₂, and fcc Au phases in the Zr₇₀Au₃₀ amorphous alloy subjected to heating at 553 K for 24 h in air.² Figure 4 shows the hydrogen *P*–*C* isotherm at 423 K of the ZrO₂ + Au nanocomposite. In the applied hydrogen pressure up to 5 MPa, no distinct absorption of hydrogen is seen, indicating that the nanoscale Au particles embedded in ZrO₂ matrix cannot absorb an appreciable amount of hydrogen. This behavior is in agreement with the previous data for Au.¹⁸



(a)



(b)

FIG. 3. (a) Dark-field TEM image and (b) selected-area electron diffraction pattern and its identified result for the melt-spun Zr₆₅Pd₃₅ subjected to heating at 553 K for 24 h in air. The dark-field image was taken from a part of (111) Pd reflection ring.

Figures 5(a) and 5(b) show the hydrogen *P*–*C* isotherms at 423 and 323 K for the ZrO₂ + Pd nanocomposite, respectively. The maximum absorbed hydrogen content in the applied hydrogen pressure of 1 MPa is about 0.7 mass% (H₂/sample). Since no distinct hydrogen absorption capacity is recognized for ZrO₂ as shown in Fig. 4, the hydrogen absorption for the nanocomposite is attributed to nanoscale Pd particles. When the hydrogen absorption is assumed to result from only Pd particles, the resulting hydrogen absorption amount for the Pd particles is evaluated to be 2.2 mass%, which is the fraction of hydrogen weight divided by only Pd content [hereafter denoted as mass% (H₂/Pd)]. The deviation at the hydrogen pressure of about 0.1 MPa appears to correspond to a plateau stage. Figure 5(b) shows the hydrogen *P*–*C* isotherm at 323 K of the nanocomposite. A distinct plateau stage is seen around the hydrogen

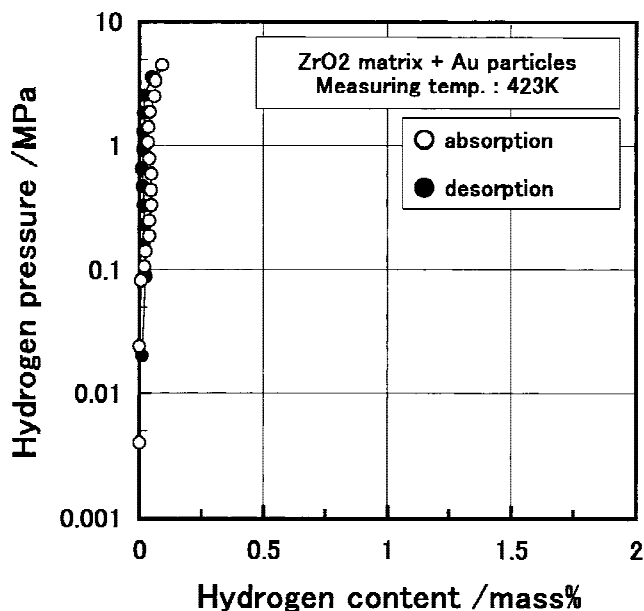


FIG. 4. Hydrogen pressure–composition (*P*–*C*) isotherm at 423 K for the ZrO₂ + Au nanocomposite prepared from an amorphous Zr₇₀Au₃₀ alloy.

pressure of 0.005 to 0.01 MPa, followed by a slow increase in absorbed hydrogen amount with an increase of applied hydrogen pressure. The maximum hydrogen absorption content reaches as high as 2.4 mass% (H₂/Pd). In Fig. 6, the hydrogen *P*–*C* isotherm relations at 323 and 423 K for pure Pd metal in bulk^{19,20} and powder with an average grain size of 0.36 μm are shown for comparison. No distinct difference in the *P*–*C* isotherm at 323 and 423 K between the bulk and the powder samples is seen. In comparison with the Pd metal in bulk and powder forms, one can notice clearly that the maximum hydrogen absorption content increases significantly for the nanocomposite. Furthermore, the desorption amount of hydrogen for the nanocomposite prepared from the Zr₆₅Pd₃₅ amorphous phase is evaluated to be 0.5 mass% (H₂/Pd) at 423 K and 1.1 mass% (H₂/Pd) at 323 K as summarized in Fig. 5.

D. Effect of Ni addition on hydrogen absorption of the nanocomposite

With the aim of increasing further the desorbed hydrogen amount, we examined the influence of Ni addition. Figure 7 shows the hydrogen *P*–*C* isotherms of the nanocomposite consisting of ZrO₂, Pd, and Ni prepared from the Zr₆₅Pd₃₀Ni₅ amorphous alloy. Although the maximum hydrogen absorption content at 323 K decreases slightly from 2.4 mass% (H₂/Pd) to 2.2 mass% [H₂/(Pd + Ni)] in the applied hydrogen pressure of 1 MPa because of the decrease in Pd content from 35 at% to 30 at%, the desorbed hydrogen amount is 1.0 mass% [H₂/(Pd + Ni)] at 423 K and 1.2 mass% [H₂/(Pd + Ni)] at

323 K, which are a little larger than those for the nanocomposite prepared from the Zr₆₅Pd₃₅ amorphous alloy [0.5 and 1.1 mass% (H₂/Pd), respectively].

E. Mechanism for large hydrogen absorption content of the nanocomposites

The particle size of Pd particles at a volume fraction of about 20% is measured to be about 10 nm. The Pd particles lie in an isolated state in the ZrO₂ matrix. This

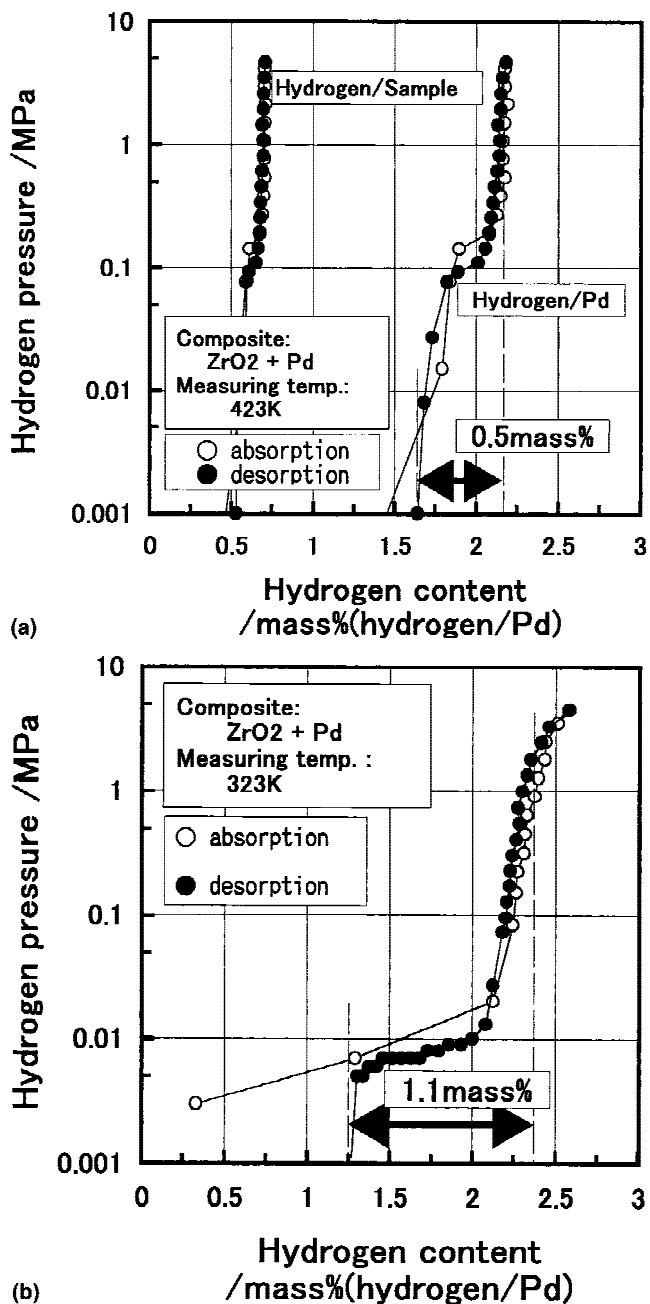


FIG. 5. Hydrogen *P*–*C* isotherm (a) at 423 K and (b) at 323 K for the ZrO₂ + Pd nanocomposite prepared from an amorphous Zr₆₅Pd₃₅ alloy.

unique structural state appears to be more appropriate for the absorption of hydrogen as compared with bulk Pd metal and ordinary Pd powder with a size of about 360 nm. In addition to the dispersion state of Pd particles in the nanocomposite, the ultrafine particle size of about 10 nm in an isolated state allows us to presume that the tremendously large area of interface of the nanoscale Pd particles has rather loose atomic configurations with higher volume fractions of vacancies which are favorable for the absorption of hydrogen. In Fig. 5, it is conceivable that a large amount of hydrogen can be trapped at the interface between Pd particles and ZrO₂ matrix, while the plateau stage becomes narrower as previously reported.^{5–8} Such a large amount of solute hydrogen can be added into the nanocomposite as a bias to the hydrogen amount required for the hydrogenation of Pd particles. That may be the reason for the large hydrogen absorption content recognized in this study. The most important engineering problem to improve the hydrogen storage properties of the nanocomposite materials is how to extract solute hydrogen from the material. The more detailed structure analysis around the nanoscale Pd particles is expected to lead to a definite clarification of the mechanism for the significant increase in hydrogen storage content in the nanocomposite structure.

IV. SUMMARY

By oxidizing the melt-spun Zr₆₅Pd₃₅ amorphous alloy at 553 K for 24 h in air, we produced a nanocomposite material consisting of nanoscale Pd particles embedded isolately in monoclinic and cubic ZrO₂ phases. Assuming

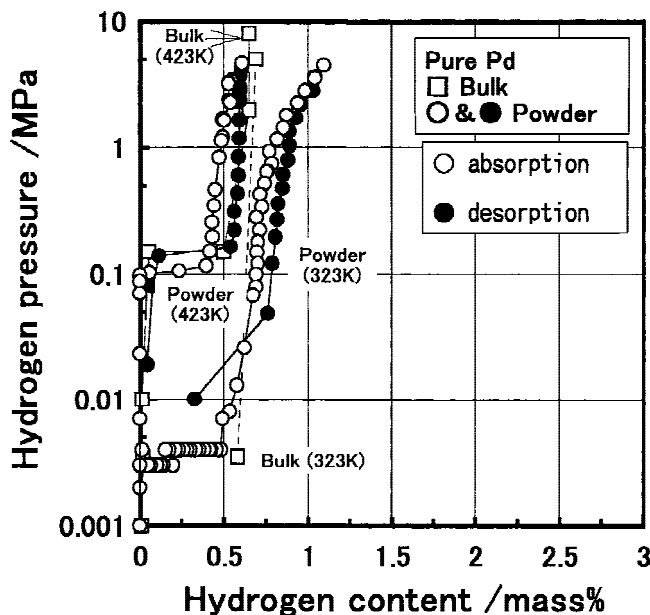


FIG. 6. Hydrogen *P*–*C* isotherms of pure Pd metal in bulk and powder forms.

that all hydrogen is absorbed by the Pd particles, the nanocomposite was found to absorb 2.4 mass% (H₂/Pd) hydrogen at 323 K and 2.2 mass% (H₂/Pd) hydrogen at 423 K in the applied hydrogen pressure of 1 MPa, which are much higher than those for the Pd metal in bulk and powder forms (0.7 and 1.2 mass%, respectively). For the nanocomposite of Pd + Ni + ZrO₂ prepared from the melt-spun Zr₆₅Pd₃₀Ni₅ amorphous ribbon, the desorbed hydrogen content was 1.0 mass% [H₂/(Pd + Ni)] at

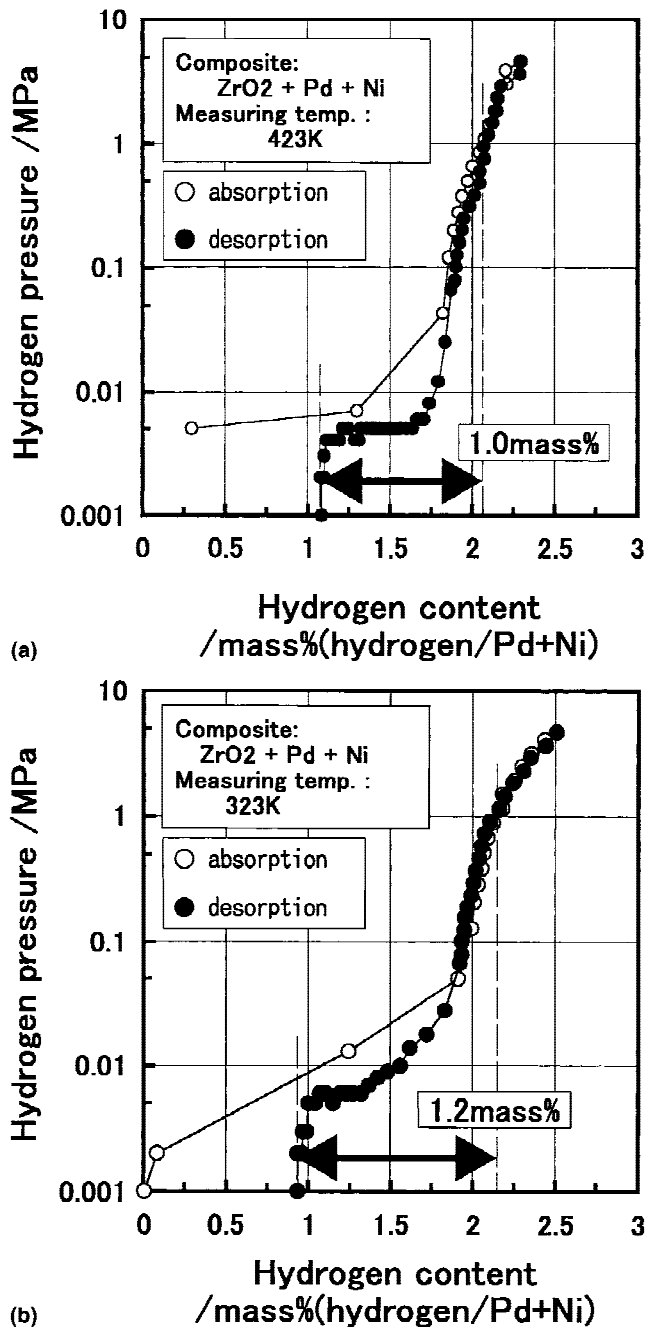


FIG. 7. Hydrogen *P*–*C* isotherms at (a) 323 and (b) at 423 K for the ZrO₂ + Pd + Ni nanocomposite prepared from an amorphous Zr₆₅Pd₃₀Ni₅ alloy.

423 K and the content increased to 1.2 mass% [H₂/(Pd + Ni)] at 323 K in the applied hydrogen pressure of 1 MPa. The increase in the hydrogen absorption amount and the rather large amount of evolution of hydrogen indicate the importance of the nanocomposite structure to fabricate a new type of hydrogen-storage material.

REFERENCES

1. H.M. Kimura, A. Inoue, and T. Masumoto, *Mater. Lett.* **14**, 232 (1992).
2. H.M. Kimura, K. Asami, A. Inoue, and T. Masumoto, *Corros. Sci.* **35**, 909 (1993).
3. H.M. Kimura, A. Inoue, T. Masumoto, and S. Itabashi, *Sci. Rep. Res. Inst. Tohoku Univ.* **A-33**, 183 (1986).
4. A. Inoue and H.M. Kimura, *J. Jpn. Inst. Light Met.* **49**, 214 (1999).
5. A. Züttel, Ch. Nuetzenadel, G. Schmid, D. Chartouni, and L. Schlapbach, *J. Alloys Compd.* **293–295**, 472 (1999).
6. A. Pundt, C. Sachs, M. Winter, M.T. Reetz, D. Fritsch, and R. Kirchheim, *J. Alloys Compd.* **293–295**, 480 (1999).
7. E. Salomons, R. Griessen, D.G. De Groot, and A. Magerl, *Europhys. Lett.* **5**, 449 (1988).
8. J.A. Eastman, L.J. Thompson, and B.J. Kestel, *Phys. Rev. B* **48**, 84 (1993).
9. M.Y. Song, *Int. J. Hydrogen Energy* **20**, 221 (1995).
10. F.E. Spada, R.C. Bowman, Jr., and J.S. Cantrell, *J. Less-Common Met.* **129**, 197 (1987).
11. J.E. Wagner, R.C. Bowman, Jr., and J.S. Cantrell, *J. Appl. Phys.* **58**, 4573 (1985).
12. A.J. Maeland, *J. Less-Common Met.* **89**, 173 (1983).
13. M.V. Nevitt, J.W. Downey, and R.A. Morris, *AIME Trans.* **218**, 1019 (1960).
14. F.J. Rotella, H.E. Flotow, D.M. Gruen, and J.D. Jorgensen, *J. Chem. Phys.* **79**, 4522 (1983).
15. I.Y. Zavalij, W.B. Yelon, P.Y. Zavalij, I.V. Saldan, and V.K. Pecharsky, *J. Alloys Compd.* **309**, 75 (2000).
16. I. Zavalij, G. Wojcik, G. Mlynarek, I. Saldan, V. Yartys, and M. Kopczyk, *J. Alloys Compd.* **314**, 124 (2001).
17. M. Paljevic and Z. Ban, *J. Less-Common Met.* **105**, 83 (1985).
18. Y.C. Huang, K. Fujita, and H. Uchida, *Bull. Jpn. Inst. Met.* **18**, 694 (1970).
19. A. Lewis, *The Palladium Hydrogen System* (Academic Press, New York and London, United Kingdom, 1967).
20. H. Frieske and E. Wicke, *Ber. Bunsen-Ges. Phys. Chem.* **77**, 48 (1973).